PCCP

ROYAL SOCIETY OF CHEMISTRY

Supporting Information

Electronic excitation spectra of cerium oxides: from ab initio dielectric response functions to Monte Carlo electron transport simulations

Andrea Pedrielli,[a,b], Pablo de Vera[a], Paolo E. Trevisanutto,[c] Nicola M. Pugno,[b,d], Rafael Garcia-Molina[e], Isabel Abril[f], Simone Taioli,[*a,g] and Maurizio Dapor[*a]

1 DOS: tests of different U_{eff} values. Band structure of bulk CeO_2 and Ce_2O_3

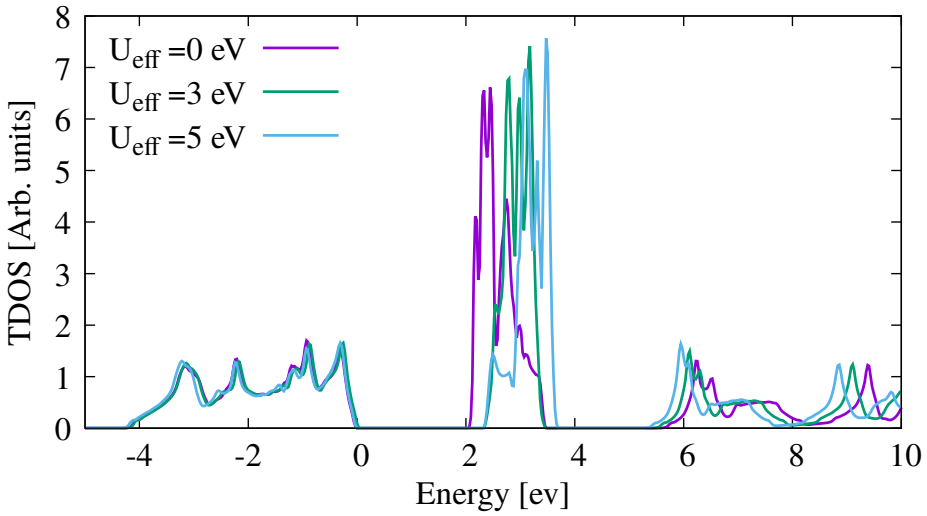

Fig. S1 Total DOS of bulk CeO_2. We show the effect of different Hubbard corrections ($U_{\text{eff}} = 0, 3, 5$ eV) to deal with the localized $4f$ states (highest peak between 2 and 4 eV). The top of the valence band is set to 0 eV.

[a] *European Centre for Theoretical Studies in Nuclear Physics and Related Areas (ECT*-FBK) and Trento Institute for Fundamental Physics and Applications (TIFPA-INFN), Trento, Italy*
[b] *Laboratory of Bio-inspired, Bionic, Nano, Meta Materials & Mechanics, Department of Civil, Environmental and Mechanical Engineering, University of Trento, Italy*
[c] *Bruno Kessler Foundation, Trento, Italy*
[d] *School of Engineering and Materials Science, Queen Mary University of London, UK*
[e] *Departamento de Física, Centro de Investigación en Óptica y Nanofísica, Universidad de Murcia, Spain*
[f] *Departament de Física Aplicada, Universitat d'Alacant, Spain*
[g] *Peter the Great St. Petersburg Polytechnic University, Russia*
* E-mail: taioli@ectstar.eu, dapor@ectstar.eu

Figure S1 shows the total density of states (TDOS) of bulk CeO_2 obtained by tuning the Hubbard correction in the commonly used range $U_{\text{eff}} = [0:5]$ eV.[1] Increasing U_{eff} results in a blueshift of the $4f$ states localized in the energy region 2 to 4 eV (the top of the valence band is shifted to 0 eV), which further opens the O2p-Ce4f gap by 0.3 eV with respect to the plain DFT-LSDA value. The broad band between -4 eV and 0 eV remains untouched by changing U_{eff}.

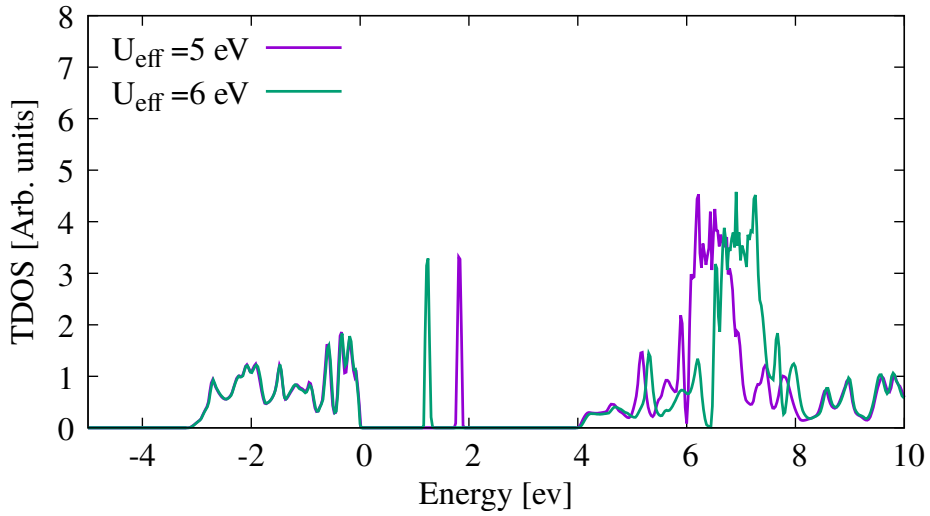

Fig. S2 Total DOS of Ce_2O_3 bulk solid. We show the effect of different Hubbard corrections $U_{\text{eff}} = 5,6$ eV to deal with the localized $4f$ states (sharp peak near to 2 eV).

In Figure S2 we report the TDOS of bulk Ce_2O_3 obtained using a Hubbard correction in the range $U_{\text{eff}} = [5:6]$ eV. In Figs. S3 and S4 we plot the band structure of CeO_2 and Ce_2O_3, respectively, calculated using DFT+U.

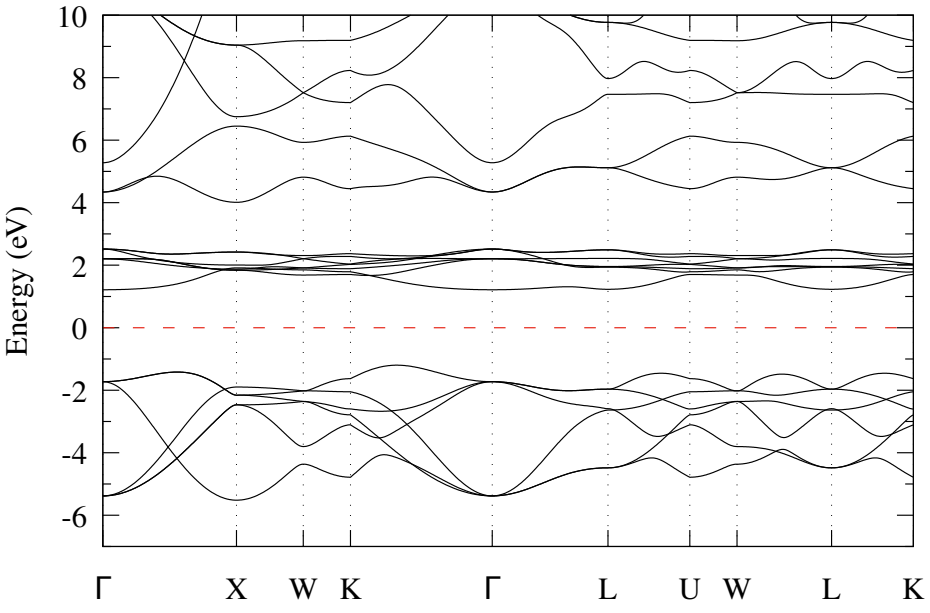

Fig. S3 Band structure of bulk CeO_2 calculated using DFT+U. The Fermi level (dashed red line) is set to the origin of the energy axis.

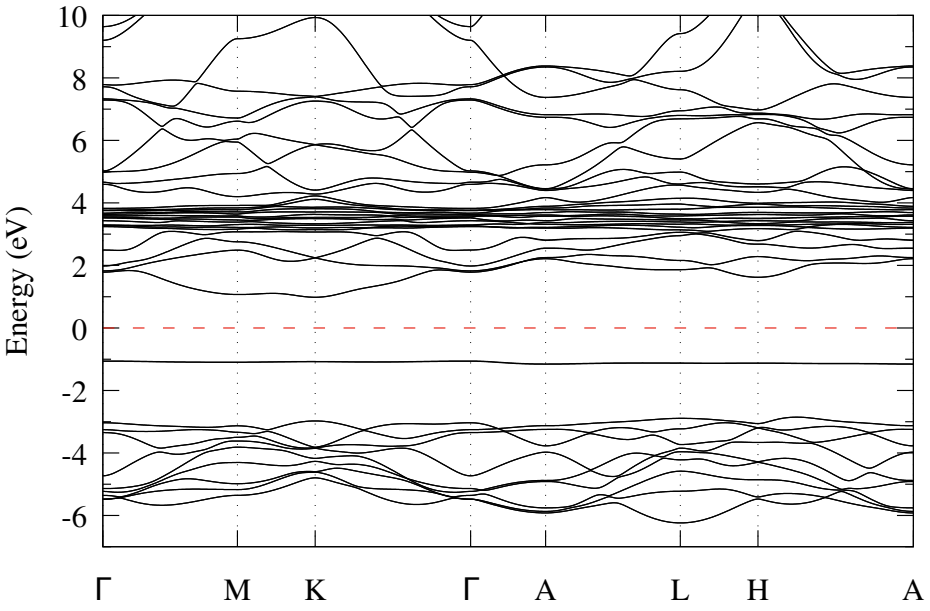

Fig. S4 Band structure of bulk Ce_2O_3 calculated using DFT+U. The Fermi level (dashed red line) is set to the origin of the energy axis.

2 ELF in the optical limit: tests of different U_{eff} values. Momentum dispersion of the ELF

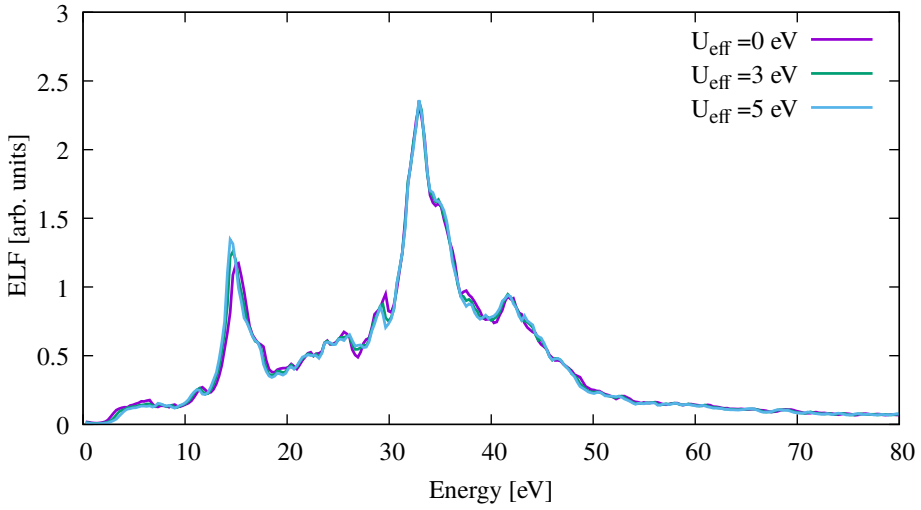

Fig. S5 ELF of bulk CeO_2 in the optical limit ($q \to 0$), calculated within the LSDA-ALDA approximation, using different values of the Hubbard correction U_{eff}.

In Fig. S5 we report the ELF of bulk CeO_2 in the optical limit ($q \to 0$) analysing the impact of different values of the Hubbard correction U_{eff}, concluding a negligible change.

The impact of different approximations on the ELF to include many-body effects using either the random phase approximation (RPA) or the ALDA kernel, with and without Local Field Effects (LFE) is shown in Fig. 4 (top panel) of the main text.

We notice that the key factor that mostly affects the accuracy is the introduction of LFE, since these effects are related to local density inhomogeneities and, thus, can be relevant in the assessment of the ELF as a function of the direction of the transferred momentum.

Furthermore, we also tested the bootstrap kernel[2], that gives results similar to RPA showing that excitonic effects are small for this system.

The *ab-initio* Bethe surface of bulk CeO_2 up to ∼170 eV, including thus the 4d transitions, is presented in Fig. S6 (top panel). It is

interesting to notice that in the $100-120$ eV range the transition peak shifts towards lower energies with increasing momentum transfer. The Bethe surface of Ce_2O_3 is also shown in Fig. S6 (bottom panel).

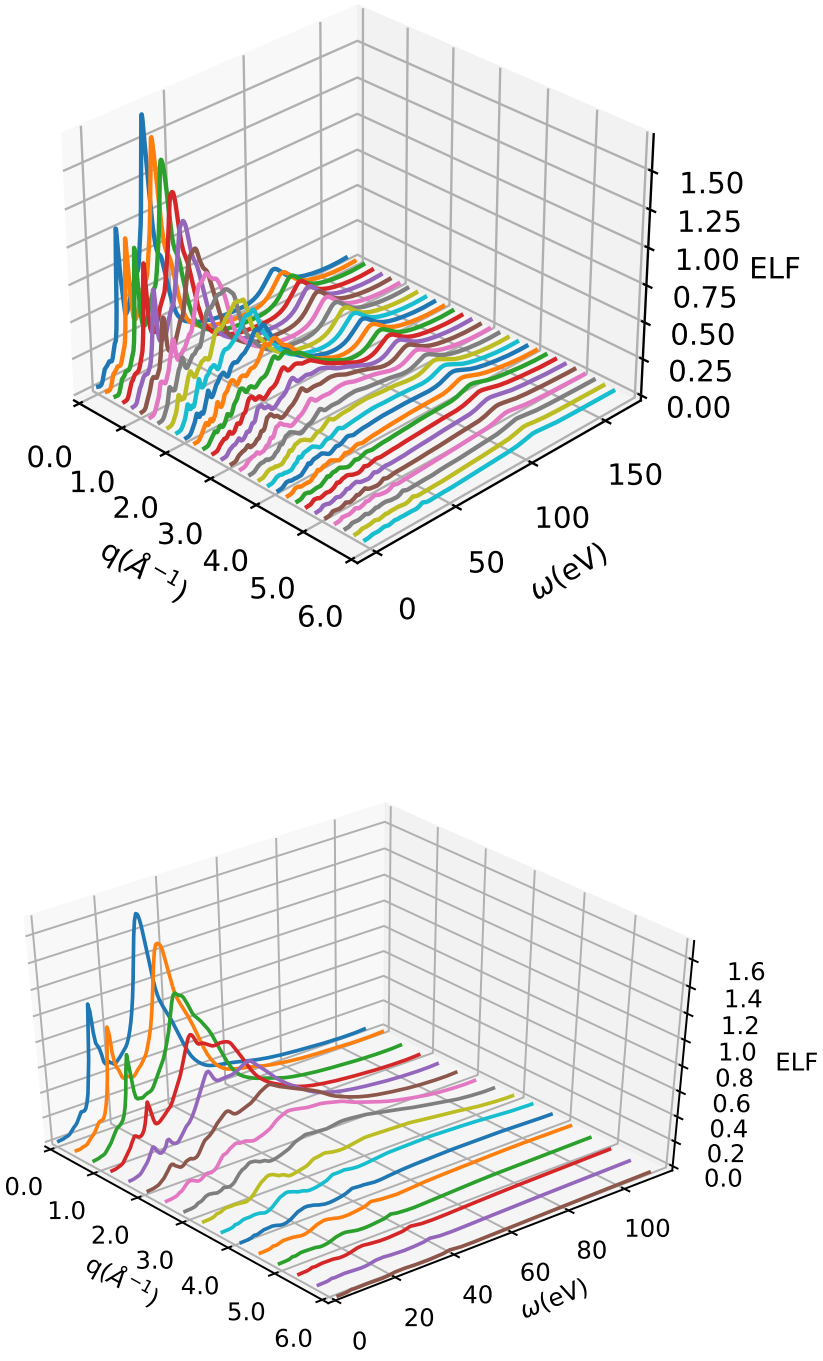

Fig. S6 ELF of bulk CeO_2 along the [111] direction (top panel) and of Ce_2O_3 along the [110] direction (bottom panel) from TDDFT calculations including LFE within ALDA.

Dependence on the direction of the momentum transfer of the ELF of bulk CeO_2 and Ce_2O_3 is reported in Figs. S7 and S8, respectively.

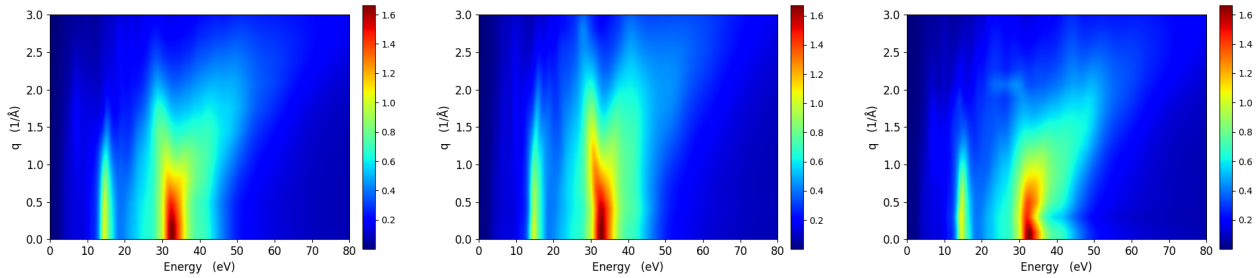

Fig. S7 Dependence of the ELF of bulk CeO_2 on different orientations of the momentum transfer vector. Left panel: [211]. Middle panel: [110]. Right panel: [111].

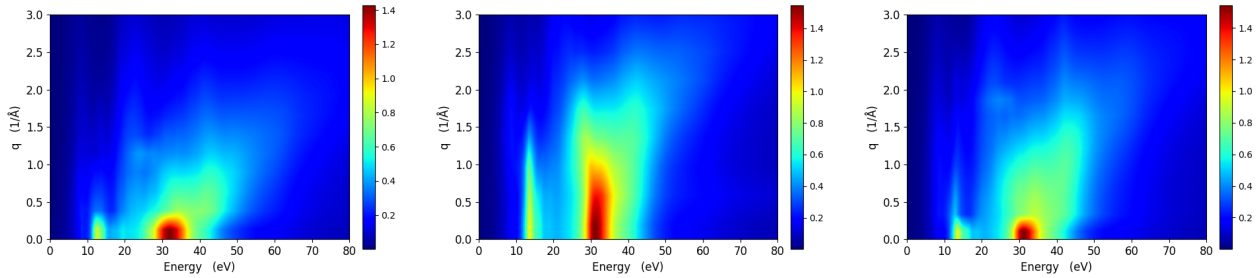

Fig. S8 Dependence of the ELF of bulk Ce_2O_3 on different orientations of the momentum transfer vector. Left panel: [001]. Middle panel: [110]. Right panel: [100].

3 Refractive index and extinction coefficient

From the knowledge of the macroscopic dielectric function $(\bar{\varepsilon}_1, \bar{\varepsilon}_2)$ of a material, one can reckon also its optical properties, such as the refraction index n and the extinction coefficient κ, as follows:

$$n = \sqrt{\frac{1}{2}\left(\sqrt{\bar{\varepsilon}_1^2 + \bar{\varepsilon}_2^2} + \bar{\varepsilon}_1\right)}, \quad \kappa = \sqrt{\frac{1}{2}\left(\sqrt{\bar{\varepsilon}_1^2 + \bar{\varepsilon}_2^2} - \bar{\varepsilon}_1\right)}, \tag{1}$$

where $\bar{\varepsilon}_{1,2}$ are the real and imaginary part of the macroscopic dielectric function, respectively.

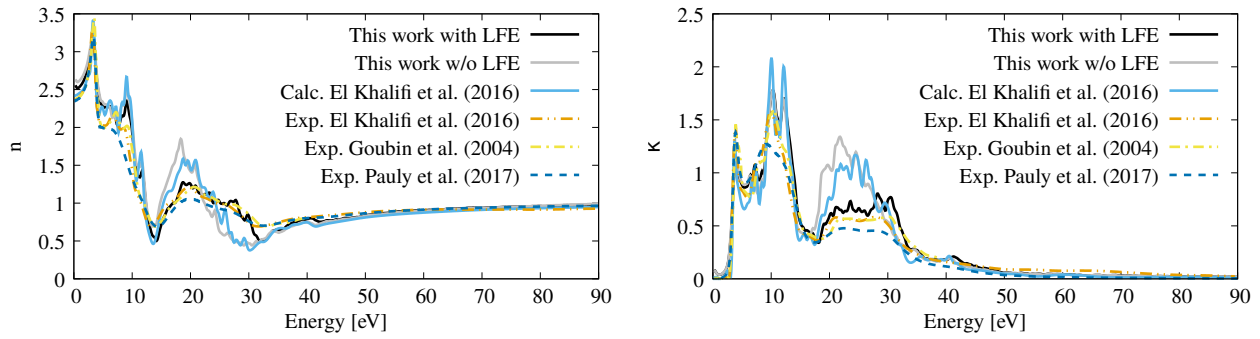

Fig. S9 Left: comparison between the refractive index of bulk CeO_2 calculated in this work and other experimental and computational studies[3–5]. Right: comparison between the extinction coefficient of bulk CeO_2 calculated in this work and other experimental and computational studies[3–5].

Using Eqns. (1), and the macroscopic dielectric matrix of eqn (4) in the main text we also calculated the refractive index and the extinction coefficient of both cerium oxides. In particular, we report in Fig. S9 the refractive index (left panel) and the extinction

coefficient (right panel) of bulk CeO_2, respectively, and their comparison with several other computational and experimental studies[3–5]. We find an overall good agreement between our calculations and previous experimental and computational data when including LFE, with an appreciable difference emerging in the range $10-30$ eV between the calculated and experimental refractive indexes and in the range $20-30$ eV between the calculated and experimental extinction coefficients when switching-off LFE. In fact, LFE strongly suppress the intensity of the third major peak and lead to a better agreement of our simulations with the experimental data.

Moreover, we report in Fig. S10 the refractive index (left panel) and the extinction coefficient (right panel) of bulk Ce_2O_3 with and without LFE.

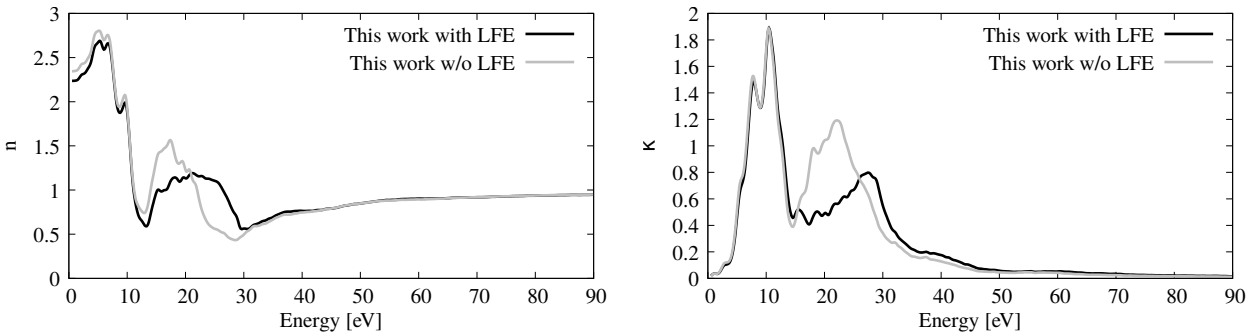

Fig. S10 Refractive index (left) and extinction coefficient (right) of bulk Ce_2O_3 with and without LFE.

4 Parameters for the MELF-GOS fitting of the ab initio optical ELF

Tables S1 and S2 report, respectively, the parameters used to fit the first principles optical ELF of CeO_2 and Ce_2O_3, by means of Eqns. (6)-(8) in the main text. In the column corresponding to Δ_i, when the word "Heaviside" appears instead of a value, it means that the function F is a Heaviside function for this function i. The criteria for the fitting, related to the fulfilment of the f-sum rules for individual transitions, are explained in the main text, sections 3.2 and 3.3.

Table S1 Parameters used in the MELF-GOS fit of the optical ELF of bulk CeO_2 (see Eqns. (6-8) of the main text).

Mermin	W_i (eV)	γ_i (eV)	A_i (eV^2)	Δ_i (eV^{-1})	$W_{\mathrm{th},i}$ (eV)
1	6.80	6.80	5.18	Heaviside	2.2
2	15.10	3.54	44.13	1.873	5.2
3	25.3	11.43	107.37	1.873	14.12
4	33.20	7.62	125.88	1.873	14.12
5	33.33	6.26	214.73	1.873	16.8
6	42.18	14.97	259.16	1.873	37.80
7	77.55	54.42	185.12	Heaviside	2.2
8	113.34	14.97	303.59	0.184	100.68
9	122.45	23.13	148.09	0.184	100.68
10	326.54	408.17	296.18	0.184	206.53
11	122.45	108.85	222.14	Heaviside	2.2

Table S2 Parameters used in the MELF-GOS fit of the optical ELF of bulk Ce_2O_3 (see Eqns. (6-8) of the main text).

Mermin	W_i (eV)	γ_i (eV)	A_i (eV^2)	Δ_i (eV^{-1})	$W_{\mathrm{th},i}$ (eV)
1	8.44	2.72	1.63	Heaviside	2.04
2	13.88	2.18	19.25	Heaviside	3.83
3	16.6	7.62	51.83	Heaviside	3.83
4	31.97	10.34	251.76	0.735	13.06
5	31.97	8.16	192.52	0.735	15.10
6	38.10	14.69	255.46	0.735	37.80
7	64.49	32.65	162.90	Heaviside	2.04
8	129.93	15.24	266.57	0.184	100.68
9	137.15	10.07	133.28	0.184	100.68
10	326.54	408.17	296.18	0.184	206.53

Notes and references

1 C. Loschen, J. Carrasco, K. M. Neyman and F. Illas, *Phys. Rev. B*, 2007, **75**, 035115.

2 S. Sharma, J. K. Dewhurst, A. Sanna and E. K. U. Gross, *Physical Review Letters*, 2011, **107**, 186401.

3 F. Goubin, X. Rocquefelte, M.-H. Whangbo, Y. Montardi, R. Brec and S. Jobic, *Chemistry of Materials*, 2004, **16**, 662–669.

4 M. El Khalifi, F. Picaud and M. Bizi, *Anal. Methods*, 2016, **8**, 5045–5052.

5 N. Pauly, F. Yubero, J. P. Espinós and S. Tougaard, *Applied Optics*, 2017, **56**, 6611.